Author/s:
Ju, Y;Cui, J;Müllner, M;Suma, T;Hu, M;Caruso, F

Title:
Engineering Low-Fouling and pH-Degradable Capsules through the Assembly of Metal-Phenolic Networks

Date:
2015-03-09

Citation:
Ju, Y., Cui, J., Müllner, M., Suma, T., Hu, M. & Caruso, F. (2015). Engineering Low-Fouling and pH-Degradable Capsules through the Assembly of Metal-Phenolic Networks. Biomacromolecules, 16 (3), pp.807-814. https://doi.org/10.1021/bm5017139.

Persistent Link:
https://hdl.handle.net/11343/54843

Engineering Low-Fouling and pH-Degradable Capsules through the Assembly of Metal-Phenolic Networks

*Yi Ju, Jiwei Cui, Markus Müllner, Tomoya Suma, Ming Hu and Frank Caruso**

ARC Centre of Excellence in Convergent Bio-Nano Science and Technology, and the Department of Chemical and Biomolecular Engineering, The University of Melbourne, Parkville, Victoria 3010, Australia.

ABSTRACT Metal-phenolic coordination chemistry provides a simple and rapid way to fabricate ultrathin films. Here, we report a facile strategy for the preparation of low-fouling and pH-degradable metal-phenolic network (MPN) capsules using a synthetic polyphenol derivative, poly(ethylene glycol) (PEG)-polyphenol, as a building block. PEG-MPN capsules exhibit reduced nonspecific protein adsorption and cell association compared with tannic acid (TA)-MPN capsules. In addition, they show faster disassembly at a biologically relevant pH (5) than TA-MPN capsules (80% in 5 h vs. 30% in 10 days). PEG-MPN capsules combine both the low fouling properties of PEG and the advantages of the MPN-driven assembly process (*e.g.*, fast assembly and pH-degradability).

KEYWORDS polymer capsules, poly(ethylene glycol), low fouling, pH-responsive disassembly, polyphenols

INTRODUCTION

Capsules with hollow structures have received widespread interest due to their application in fields as diverse as biomedical imaging, synthetic biology, and drug delivery.[1-5] The deposition of thin films on sacrificial template particles, followed by the selective removal of templates, is a robust approach to fabricate capsules with defined geometries. Recently, we developed a one-step approach to assemble phenolic thin films on a variety of substrates by forming coordination complexes between metal ions (*e.g.*, Fe^{III}) and natural polyphenols (*e.g.*, tannic acid (TA), (-)-Epigallocatechin gallate (EGCG)), termed metal-phenolic networks (MPNs).[6] This MPN-driven assembly is straightforward and allows rapid film assembly for capsule preparation, and is an alternative approach to polyphenol-based layer-by-layer coatings.[7,8] Furthermore, the incorporation of different metal species into MPNs allows facile functionalization of capsules for a variety of applications, such as positron emission tomography ($^{64}Cu^{II}$), magnetic resonance imaging (Gd^{II}), and catalytic hydrogenation of quinoline (Rh^{III}).[9] However, these earlier studies for engineering MPN capsules mainly focused on naturally derived polyphenols. While natural polyphenols are readily available and inexpensive,[10] they also exhibit strong nonspecific interactions with biological systems.[11-14] MPN capsules derived from natural polyphenols can be nonspecifically internalized by cells *in vitro* or rapidly accumulated in organs *in vivo*,[9] which in turn may limit their application in certain biological systems, for example, where long blood circulation times are required.

Inspired by the pristine properties of natural polyphenols, many functional polyphenol derivatives have been introduced by conjugating phenolic ligands to (bio)macromolecules.

Hyaluronic acid (HA)-catechol conjugates, for example, have been used to build two-dimensional cell-engineering hydrogels through the oxidation of catechol groups.[15] Phenolic groups were also introduced to dendritic polyglycerol to form films through covalent crosslinking or ion-based coordination crosslinking.[16] Holten-Andersen *et al*. produced a self-healing hydrogel based on the coordination of a 4-arm-poly(ethylene glycol) (PEG)-catechol and Fe^{III}, which cross-linked to networks with near covalent stiffness.[17] PEG is a well-recognized stealth material.[18,19] The low-fouling properties of PEG and the advances in producing artificial polyphenols make it interesting to design synthetic PEG-based TA analogues and to combine them with the advantages of the MPN-driven assembly process.

Herein, we report the template-assisted assembly of low-fouling and pH-degradable capsules based on coordination between metal ions and a synthetic polyphenol derivative (Scheme 1). PEG-polyphenol was synthesized by conjugating catechol groups onto each terminus of an 8-arm-PEG. PEG-MPNs were assembled by adding Fe^{III} into a PEG-polyphenol solution, followed by increasing the pH to form metal-phenolic coordination complexes. This approach offers a number of distinct advantages: (i) PEG-MPN capsules are obtained via rapid assembly due to the high surface binding affinity and metal chelating properties of phenolic groups; (ii) PEG-MPN capsules exhibit significantly higher resistance to nonspecific protein adsorption and cellular association due to the intrinsic low-fouling properties of PEG; and (iii) the use of catechol groups allows fine-tuning of the pH-degradability of MPN capsules, leading to disassembly in a physiologically relevant acidic environment (pH 5), which allows the controlled release of cargo for potential intracellular drug delivery.

Scheme 1. Assembly of PEG-MPN capsules. PEG-MPN capsules were prepared by adding PEG-polyphenol into a suspension of $CaCO_3$ particles, followed by adding Fe^{III}, increasing the pH, and dissolving the templates. The assembly of PEG-MPN capsules is based on the coordination between PEG-polyphenol and Fe^{III}.

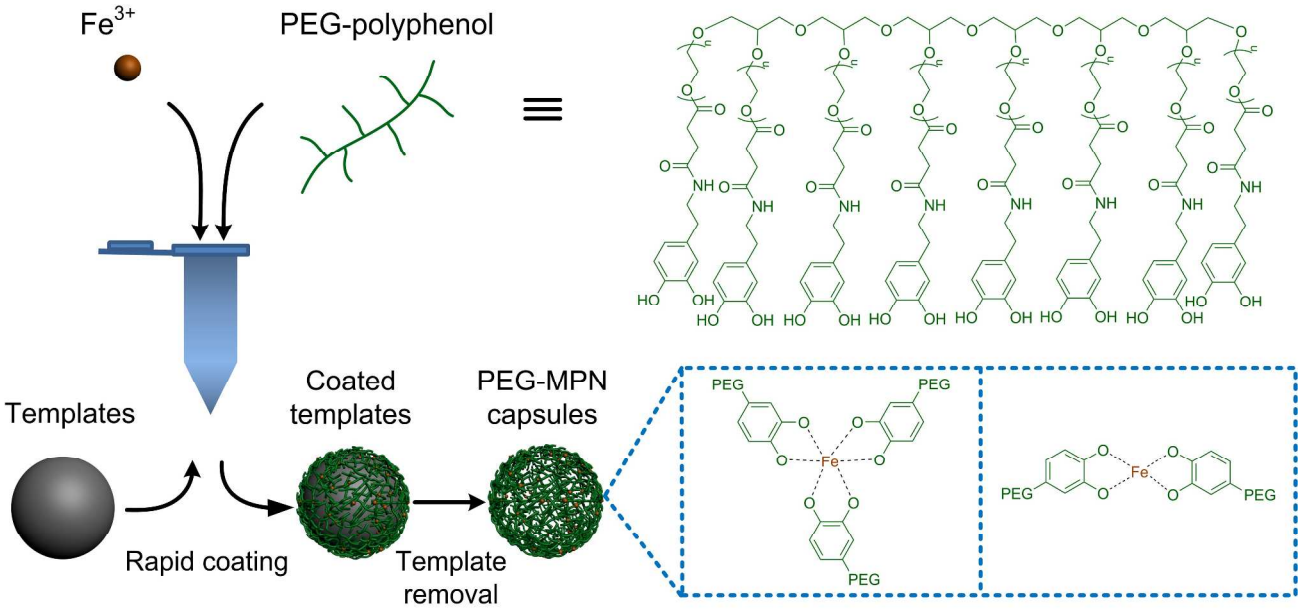

EXPERIMENTAL SECTION

Materials. 8-arm-poly(ethylene glycol) succinimidyl succinate (8-arm-PEG-NHS, hexaglycerol core, M_w ~10 kDa) was purchased from JenKem Technology (USA). Iron (III) chloride hexahydrate ($FeCl_3 \cdot 6H_2O$), tannic acid (TA), dopamine hydrochloride, tris(hydroxymethyl)aminomethane (TRIS), 3-(N-morpholino) propanesulfonic acid (MOPS), calcium chloride ($CaCl_2$), sodium carbonate (Na_2CO_3), phosphate buffered saline (PBS) tablet, dextran-fluorescein isothiocyanate ($dextran_{FITC}$, 2000 kDa), ethylenediaminetetraacetic acid (EDTA), poly(ethyleneimine) (PEI, M_w 25 kDa), 2,3-bis[2-Methoxy-4-nitro-5-sulfophenyl]-2H-tetrazolium-5-carboxyanilide inner salt (XTT), anhydrous *N*,*N*-dimethylformamide (DMF), triethylamine (TEA), anhydrous dimethyl sulfoxide (DMSO), deuterium oxide (D_2O), human

blood serum (HBS), and bovine serum albumin (BSA) were purchased from Sigma-Aldrich (USA). Poly(methacrylic acid) (PMA, M_w 15 kDa) was purchased from Polysciences (USA). Dulbecco's phosphate-buffered saline (DPBS), Dulbecco's modified Eagle's medium (DMEM), Alexa Fluor 488 (AF488) cadaverine, wheat germ agglutinin Alexa Fluor 594 conjugate (WGA594) and Hoechst 33342 were obtained from Life Technologies (USA). All chemicals were used as received without further purification. The pH values of all solutions were measured with a Mettler-Toledo MP220 pH meter. High-purity water (Milli-Q water) with a resistivity greater than 18.2 MΩ cm was obtained from a three-stage Millipore Milli-Q plus 185 purification system (Millipore Corporation, USA). All aqueous solutions were filtered with 200 nm diameter membranes before use.

PEG-Polyphenol Synthesis. 100 mg (10^{-5} mol) of 8-arm-PEG-NHS (10 kDa) and 76 mg (4×10^{-4} mol) of dopamine hydrochloride (1:5 PEG terminal: dopamine molar ratio) were separately dissolved in 1 mL and 0.5 mL of degassed anhydrous DMF, respectively. The two solutions were then mixed and degassed by argon bubbling. Subsequently, 66.5 μL (4.8×10^{-4} mol) of anhydrous TEA (1:1.2 TEA: dopamine molar ratio) was added. The mixture was stirred at room temperature under argon for 12 h. The reaction mixture was purified by dialysis (~3500 MWCO; Thermo Fisher Scientific, USA) for three days against 3 L of pre-degassed Milli-Q water (adjusted to pH 3.5), followed by lyophilization to obtain PEG-polyphenol as a white powder. To fluorescently label the PEG-polyphenol, 0.32 mg (5×10^{-7} mol) of AF488 cadaverine (20:1 PEG: AF488-cadaverine molar ratio) in anhydrous DMSO was added into a dopamine and 8-arm-PEG-NHS solution, as described above, in a one-pot reaction. The resultant product was a light yellow colored powder.

PEG-Polyphenol Characterization. The chemical structure of the products and the efficiency of the modification were determined by nuclear magnetic resonance (^{1}H NMR) spectroscopy using a 400 MHz Varian INOVA system in D_2O at 25 °C (Figure S1). The efficiency of modification was determined by comparing the integral value of methylene protons of PEG at δ = 3.65 ppm to the aromatic protons of catechol at δ = 6.6 to 7.0 ppm.

$CaCO_3$ Template Synthesis. $CaCO_3$ template particles were synthesized according to a previously reported procedure.[20] 15 mL of a 0.38 M $CaCl_2$ solution was rapidly added to an equal volume of a 0.38 M Na_2CO_3 solution with vigorous mixing. After stirring for 60 s, the precipitate was filtered, washed extensively with Milli-Q water and acetone, and then dried in air. The synthesized $CaCO_3$ particles were monodisperse and spherical with a diameter of 3.2 ± 0.3 μm. The cargo-loaded $CaCO_3$ templates were synthesized by co-precipitation of $CaCO_3$ and cargo (BSA_{AF488} or $dextran_{FITC}$) according to a previously reported procedure.[21] Typically, 625 μL of 1 M $CaCl_2$ was added to 5 mL of BSA_{AF488} or $dextran_{FITC}$ (2000 kDa) solution (1 mg mL^{-1}), followed by 625 μL of 1 M Na_2CO_3. After vigorous stirring for 1 min, the precipitate was collected by centrifugation (800 *g*, 30 s) and washed three times with Milli-Q water. This procedure led to monodisperse, cargo-loaded $CaCO_3$ particles. BSA_{AF488}- and $dextran_{FITC}$-loaded CaCO3 particles have diameters of 2.4 ± 0.2 μm and 3.5 ± 0.3 μm, respectively.

PEG-MPN Capsule Synthesis. The standard protocol for the synthesis of PEG-MPN capsules was followed: 8 mg of $CaCO_3$ particles with a diameter of 3.2 ± 0.3 μm were suspended in 800 μL of Milli-Q water. 800 μL of PEG-polyphenol solution (10 mg mL^{-1}) and 1.72 mL of $FeCl_3 \cdot 6H_2O$ solution (1 mg mL^{-1}) were successively added to the aqueous $CaCO_3$ particle suspension (corresponding to approximate molar ratios of 1:1 between catechol and Fe^{III}). The suspension was vigorously stirred for 2 min after each addition of PEG-polyphenol and

$FeCl_3 \cdot 6H_2O$ solutions. Subsequently, 4 mL of TRIS buffer (50 mM, pH 8.5) was added to raise the pH, followed by vigorous stirring. The final concentrations of $CaCO_3$ particles, PEG-polyphenol and $FeCl_3 \cdot 6H_2O$ were about 1 mg mL^{-1}, 1 mg mL^{-1} and 0.23 mg mL^{-1}, respectively. Next, the particles were washed three times with Milli-Q water by centrifugation (3000 *g*, 3 min) to remove excess PEG-polyphenol and $FeCl_3$. To obtain PEG-MPN capsules, the particles were washed with EDTA (200 mM, pH 8.0) to dissolve the $CaCO_3$ templates and then washed with Milli-Q water by centrifugation (3000 *g*, 7 min). To fluorescently label the capsules, AF488-labeled PEG-polyphenol was used to prepare PEG-MPN capsules. To load cargo into the capsules, $dextran_{FITC}$- or BSA_{AF488}-loaded $CaCO_3$ particles were prepared (as described above) and used as templates to assemble PEG-MPN capsules.

TA-MPN Capsule Synthesis. TA-MPN capsules were prepared following a previously published protocol.[6] 8 mg of $CaCO_3$ particles with a diameter of 3.2 ± 0.3 μm were suspended in 3.8 mL of Milli-Q water. 40 μL of TA solution (40 mg mL^{-1}) and 40 μL of $FeCl_3 \cdot 6H_2O$ solution (10 mg mL^{-1}) were successively added to the aqueous $CaCO_3$ particle suspension (corresponding to approximate molar ratios of 1:1.6 between TA and Fe^{III}). The suspension was vigorously stirred for 2 min after each addition of TA and $FeCl_3$ solutions. Subsequently, 4 mL of MOPS buffer (20 mM, pH 8.0) was added to raise the pH, followed by vigorous stirring. The final concentrations of $CaCO_3$ particles, TA and $FeCl_3 \cdot 6H_2O$ were 1 mg mL^{-1}, 0.2 mg mL^{-1}, and 0.05 mg mL^{-1}, respectively. Next, the pellets were washed three times with Milli-Q water by centrifugation (2000 *g*, 3 min) to remove the excess TA and $FeCl_3$. To obtain TA-MPN capsules, particles were washed with EDTA (200 mM, pH 8.0) to dissolve the $CaCO_3$ templates and then washed with Milli-Q water by centrifugation (3000 *g*, 5 min). To fluorescently label capsules, BSA_{AF488}-loaded $CaCO_3$ particles were used as templates to assemble the capsules.

PEG-MPN Capsule Characterization. Differential interference contrast (DIC) and fluorescence microscopy images were obtained using an inverted Olympus IX71 microscope (Olympus, Japan). Atomic force microscopy (AFM) analysis was performed in air using a JPK NanoWizard II BioAFM (JPK Instruments AG, Germany) with tapping-mode cantilevers (46 $N \cdot m^{-1}$, NSC15/ALBS, MikroMasch, USA). The film thicknesses of 12 capsules were analyzed using JPK SPM data processing software (v.4.4.28) and then averaged to determine the mean single-layer thickness of each sample. The structure and metal content of capsules were analyzed by transmission electron microscopy (TEM) and energy dispersive X-ray spectroscopy (EDX) by using a FEI Tecnai TF20 instrument (FEI, USA) with an operation voltage of 200 kV. The morphology of capsules was analyzed by scanning electron microscopy (SEM) images obtained with a Philips XL30 field-emission scanning electron microscope (Philips, Netherlands) operated at a voltage of 2.0 kV and a spot size of 2. Capsule suspensions were dropped and air-dried on Piranha-cleaned glass slides, formvar-carbon-coated gold grids and Piranha-cleaned silicon wafers for AFM, TEM, and SEM experiments, respectively. *Caution: Piranha solution is strongly oxidizing and corrosive! Extreme care should be taken during preparation and use!* The SEM samples were sputter coated with gold before measurement.

PEG-Polyphenol−Fe Complexes in Solution. The ultraviolet to visible (UV-Vis) absorption spectra of solutions of PEG-polyphenol with $FeCl_3$ were obtained using a Varian Cary 4000 UV-Vis spectrophotometer (Varian, USA). 0.5 mL of PEG-polyphenol solution (10 mg mL^{-1}) and 1.15 mL of $FeCl_3 \cdot 6H_2O$ solution (1 mg mL^{-1}) were subsequently added into 3.35 mL of Milli-Q water, followed by vigorous stirring. The final concentrations of PEG-polyphenol and $FeCl_3 \cdot 6H_2O$ were 1 mg mL^{-1} and 0.23 mg mL^{-1}, respectively (corresponding to molar ratios of 1:1 between catechol and Fe^{III}). The pH of the solution was increased by titration with 0.5 M

NaOH. The absorbance of the mixed solution of PEG-polyphenol and $FeCl_3$ was measured immediately after adjusting the pH.

PEG-MPN Capsule Disassembly. 1 mL of AF488-labeled PEG-MPN capsules (prepared from D = 3.2 ± 0.3 μm $CaCO_3$ templates, ~1.9×10^7 capsules mL^{-1}) was incubated in phosphate buffer (50 mM, pH 7.4) or sodium acetate buffer (50 mM, pH 5.0) in an Eppendorf thermostated shaker (Eppendorf, Germany) at 37 °C with mild shaking (600 rpm). At designated time points, the capsule suspensions were diluted with Milli-Q water and the number of capsules was counted using an Apogee A50-Micro flow cytometer (Apogee Flow Systems, UK).

Cargo Release. The fluorescence intensity of $dextran_{FITC}$- or BSA_{AF488}-loaded PEG-MPN capsules was monitored with an Apogee A50-Micro flow cytometer at an excitation wavelength of 488 nm. 1 mL of $dextran_{FITC}$-loaded PEG-MPN capsules (prepared from D = 3.5 ± 0.3 μm $dextran_{FITC}$-loaded $CaCO_3$ templates, ~1.5×10^8 capsules mL^{-1}) or BSA_{AF488}-loaded PEG-MPN capsules (prepared from D = 2.4 ± 0.2 μm BSA_{AF488}-loaded $CaCO_3$ templates, ~2.9×10^8 capsules mL^{-1}) in Na_2HPO_4 (50 mM, pH 7.4) or sodium acetate (50 mM, pH 5.0) was incubated in an Eppendorf thermostated shaker at 37 °C with mild shaking (600 rpm). At designated time points, the mean fluorescence intensity of $dextran_{FITC}$ or BSA_{AF488} from the capsules was measured to determine the release of $dextran_{FITC}$ or BSA_{AF488} from the capsules.

Cargo Loading Capacity. The total amount of $dextran_{FITC}$ encapsulated in the PEG-MPN capsules was determined by fluorescence spectrophotometry. Spectra were obtained using a Horiba Fluorlog-3 Model FL3-22 spectrofluorometer (Horiba Jobin Yvon Inc., USA) equipped with a HgXe lamp (increment size, 1 nm; excitation and emission slit widths, 5 nm). 1 mL of $dextran_{FITC}$-loaded PEG-MPN capsules (prepared from D = 3.5 ± 0.3 μm $dextran_{FITC}$-loaded $CaCO_3$ templates, ~1.5×10^8 capsules mL^{-1}) was disassembled by incubation in sodium acetate

(50 mM, pH 5.0) in an Eppendorf thermostated shaker at 37 °C with shaking (600 rpm) for 20 h. After incubation, the fluorescence intensity of $dextran_{FITC}$ in the solution was measured. The concentration of $dextran_{FITC}$ was calculated based on a standard curve of fluorescence intensity versus concentration calibrated with a set of $dextran_{FITC}$ solutions of different concentrations at pH 5.0. The initial concentration of capsules was measured with an Apogee A50-Micro flow cytometer. The loading amount of $dextran_{FITC}$ was expressed as pg per capsule.

QCM Measurement of Protein Adsorption on Planar Films. Before use, QCM chips (gold-coated 9 MHz AT-cut crystals with a diameter of 4.5 mm, Kyushu Dentsu, Japan) were cleaned with Piranha solution (7:3 v/v 97% sulfuric acid: 30% hydrogen peroxide) for 30 s, rinsed with Milli-Q water, and dried by nitrogen gas. *Caution: Piranha solution is strongly oxidizing and corrosive! Extreme care should be taken during preparation and use!* PEG-MPN films were coated on the QCM chips using the following protocol: QCM chips were soaked in Milli-Q water in a 5 mL tube. Solutions of PEG-polyphenol, $FeCl_3 \cdot 6H_2O$ and TRIS buffer (50 mM, pH 8.5) were subsequently added to this aqueous solution, followed by vigorous stirring for a few minutes after each addition. The final concentration of PEG-polyphenol and $FeCl_3 \cdot 6H_2O$ were 1 mg mL^{-1} and 0.23 mg mL^{-1}, respectively, in 1 mL of Milli-Q water. Then, the chips were thoroughly washed with Milli-Q water and dried by nitrogen gas. To perform the protein adsorption studies, PEG-MPN film-coated QCM chips were incubated with undiluted human blood serum (HBS) at 37 °C for 1 h. After incubation, the chips were washed with PBS and Milli-Q water and dried by nitrogen gas flow. For comparison, TA-MPN, PEI, and PMA films were coated on QCM chips and then incubated with HBS under the same conditions. The deposition of TA-MPN films on QCM chips was performed using a previously reported method.[6] Solutions of TA, $FeCl_3 \cdot 6H_2O$ and MOPS (20 mM, pH 8.0) were sequentially added to the

aqueous solution containing a QCM chip, followed by vigorous stirring for a few minutes after each addition. The final concentration of TA and $FeCl_3 \cdot 6H_2O$ were 0.2 mg mL^{-1} and 0.05 mg mL^{-1}, respectively, in 1 mL of Milli-Q water. MPN-coated chips were extensively washed with Milli-Q water, dried by nitrogen gas flow, and immediately used for the protein adsorption studies. PEI films were coated on QCM chips by incubating the chips with 1 mg mL^{-1} of PEI solution containing 0.5 M NaCl for 10 min at 25 °C. The chips were then thoroughly washed with Milli-Q water and dried by nitrogen gas. To obtain PMA films, PEI-coated QCM chips were subsequently incubated with 1 mg mL^{-1} of PMA solution for 10 min at 25 °C, followed by thoroughly washing with Milli-Q water and drying with nitrogen gas.

QCM measurements were performed using a custom made crystal oscillator powered by an Agilent E3620A power supply (Agilent Technologies, USA). The resonant frequency was measured using an Agilent 53131A universal counter (Agilent Technologies, USA).[22] The piezoelectric quartz crystal changes its fundamental oscillation frequency (F_0) as mass (m) is deposited onto (or depleted from) the surface. According to the Sauerbrey equation, the resonant frequency shift (ΔF) of a QCM is proportional to the mass change (Δm):[23]

$$\Delta F = -\frac{2F_0^2}{A(\mu_q \rho_q)^{\frac{1}{2}}} \Delta m$$

where μ_q is the shear modulus of the quartz (2.947×10^{13} g m^{-1} s^{-2}), ρ_q is the density of the quartz (2.648×10^6 g m^{-3}), F_0 is the operating frequency of the crystals (9×10^6 Hz), and A is the piezoelectric area of the electrode (1.59×10^{-5} m^2).

Protein Fouling of Capsules. PEG-MPN capsules and MPN capsules were washed in PBS before the protein fouling test. An equal number of unlabeled capsules of each sample (prepared from D = 3.2 ± 0.3 μm $CaCO_3$ templates, ~1.3×10^7) was incubated with 200 μL of protein solution (50% AF488-labeled HBS or 5 mg mL^{-1} AF488-labeled BSA in PBS) at 37 °C for 1 h.

Subsequently, the capsules were washed with PBS to remove the unbound protein. The relative amount of adsorbed protein on the capsules was measured with an Apogee A50-Micro flow cytometer by analyzing the fluorescence intensity of the capsules. Each experiment was performed in triplicate.

Cell Culture. Human cervical carcinoma cells (HeLa, ATCC, USA) were maintained at 37 °C, with 5% CO_2 and 95% relative humidity in DMEM containing 10% heat-inactivated fetal bovine serum (FBS) and 2 mM L-glutamine.

Capsule Cytotoxicity Assay. Cell viability was measured via an XTT assay. HeLa cells were seeded into a 96-well plate at a cell density of ~5×10^3 cells per well and incubated for 24 h to allow cellular adhesion on substrates. A different number of PEG-MPN capsules (prepared from D = 3.2 ± 0.3 μm $CaCO_3$ templates) were incubated with cells for 48 h. After incubation, the cell viability assay was conducted according to the manufacturer's protocol. The absorbance at 450 nm was determined using an Infinite M200 microplate reader (Tecan, Switzerland). The cell viability was expressed as a percentage to the absorbance of non-treated cells.

Cellular Association Studies *via* Flow Cytometry. HeLa cells were trypsinized, counted, and seeded into a 24-well plate at a cell density of ~4×10^4 cells per well. Subsequently, the seeded cells were incubated for 12 h to allow cellular adhesion on substrates. PEG-MPN capsules loaded with BSA_{AF488} (prepared from D = 2.4 ± 0.2 μm BSA_{AF488}-loaded $CaCO_3$ templates) and TA-MPN capsules loaded with BSA_{AF488} (prepared from D = 2.4 ± 0.2 μm BSA_{AF488}-loaded $CaCO_3$ templates) were incubated with cells at a capsule-to-cell ratio of 50:1 for up to 24 h. After incubation, the cells were gently washed twice with DPBS, lifted with trypsin and counted with an Apogee A50-Micro flow cytometer. The cellular association of

capsules was evaluated by using the percentage of cells that showed fluorescence. Each experiment was performed in triplicate.

Cellular Association Studies *via* Deconvolution Microscopy. HeLa cells were seeded at ~3 × 10^4 cells per well into 8-well Lab-Tek chambered coverglass slides (Thermo Fisher Scientific, USA) and incubated overnight. PEG-MPN capsules loaded with BSA_{AF488} (prepared from D = 2.4 ± 0.2 μm BSA_{AF488}-loaded $CaCO_3$ templates) and TA-MPN capsules loaded with BSA_{AF488} (prepared from D = 2.4 ± 0.2 μm BSA_{AF488}-loaded $CaCO_3$ templates) were incubated with cells at a capsule-to-cell ratio of 50:1 for 24 h, followed by washing with DPBS twice. Cells were fixed with 3% paraformaldehyde in DPBS for 30 min at 37 °C, then stained with Hoechst 33342 (0.1 mg mL^{-1}) for 10 min at room temperature and stained with WGA594 (10 μg mL^{-1}) for 5 min at room temperature. Imaging to monitor the cellular association of capsules was performed using an Applied Precision DeltaVision OMX V4 Blaze Structured Illumination Microscope (Applied Precision, USA) operating in conventional mode with a 60× objective. The images were deconvolved by Softworx 6.1.1.

RESULTS AND DISCUSSION

Synthesis of PEG-Polyphenol. To mimic the structure of natural polyphenols, we synthesized a polyphenol derivative, PEG-polyphenol (Scheme 1), with an 8-arm brush structure by conjugation of 8-arm-PEG-NHS (10 kDa) and dopamine. ^{1}H-NMR spectroscopy was used to determine the efficiency of the modification by comparing the integral value of methylene protons of PEG with the aromatic protons of catechol (Figure S1). Accordingly, around 98% of the PEG end-groups were modified with catechol groups; this is higher than previously reported modification efficiencies.[24-26] The presence of multiple catechol groups allows the formation of MPNs mediated by multivalent coordination bonding.

Stoichiometric Transition of PEG-Polyphenol−Fe Complexes. To examine the capability of PEG-polyphenol to form coordination complexes with Fe^{III}, PEG-polyphenol and $FeCl_3$ solutions were mixed at different pH values. The color of the mixed PEG-polyphenol and Fe^{III} solution changed progressively from colorless, green, blue, purple to red when the pH was gradually increased from 3 to 11 (Figure S2). This color change is attributed to the transition of coordination complexes from mono- to bis- to tris-catechol complexes. UV-Vis spectrophotometry was then employed to study the stoichiometric transitions of PEG-polyphenol−Fe^{III} complexes at different pH values: the mono-complex dominated at pH <5.6, the bis-complex at 5.6 < pH < 9.1, and the tris-complex at pH > 9.1 (Figure S2), which is consistent with previous reports.[17,27] The pH-dependent stoichiometry of the PEG-polyphenol−Fe^{III} complex allows the formation of stable coordination networks at physiological pH, while promoting their disassembly under mild acidic conditions.

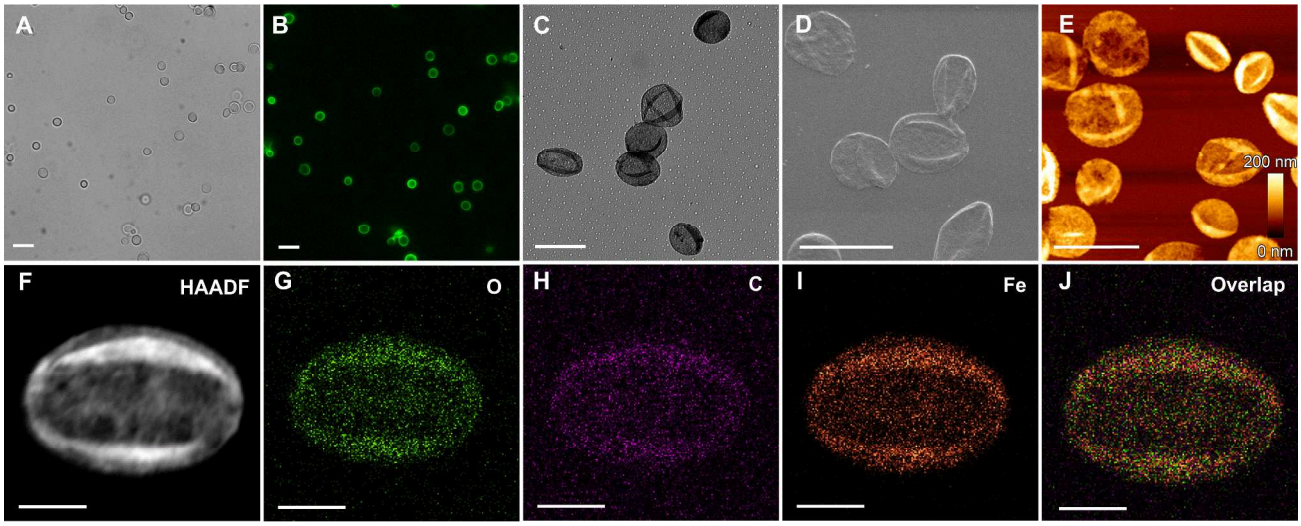

Figure 1. (A) Differential interference contrast microscopy, (B) fluorescence microscopy, (C) transmission electron microscopy, (D) scanning electron microscopy, and (E) atomic force microscopy images of PEG-MPN capsules; (F-J) corresponding energy-dispersive X-ray elemental mapping of PEG-MPN capsules. Scale bars are 5 μm (A-E) and 1 μm (F-J).

Synthesis and Characterization of PEG-MPN Capsules. To prepare PEG-MPN capsules, a PEG-polyphenol (AF488-labeled for fluorescence imaging) solution was mixed with an aqueous suspension of $CaCO_3$ templates. (Characterization of the templates is elaborated on below.) Due to the high surface binding affinity of catechol groups,[28] PEG-polyphenol rapidly coated the templates. Subsequent addition of Fe^{III} and increasing the pH caused instantaneous cross-linking of the metal-phenolic networks. Following removal of the $CaCO_3$ templates by EDTA (200 mM, pH 8.0), monodisperse, spherical PEG-MPN capsules were obtained, as observed by differential interference contrast (DIC) microscopy and fluorescence microscopy (Figure 1A,B). After air-drying, PEG-MPN capsules collapsed and exhibited folds and creases, which is a typical feature of hollow polymer capsules,[6] as confirmed by transmission electron microscopy (TEM), scanning electron microscopy (SEM) and atomic force microscopy (AFM) (Figure 1C-E). From AFM height analysis, the single-layer thickness of PEG-MPN capsules is 20 ± 2 nm (Figure S3). The presence of Fe in the PEG-MPN capsules was confirmed by energy-dispersive X-ray (EDX) spectroscopy (Figure S4). EDX mapping analysis (Figure 1F-J) showed that the Fe distribution patterns match closely with oxygen and carbon elemental patterns, as well as high-angle annular dark-field (HAADF) images, indicating that Fe is associated with PEG-polyphenol and uniformly distributed in the PEG-MPN films. Without the addition of Fe^{III}, capsules were not obtained, corroborating that metal-phenolic coordination is the driving force for PEG-MPN formation. In addition, the cytotoxicity of the PEG-MPN capsules was found to be negligible, according to an XTT assay (Figure S5).

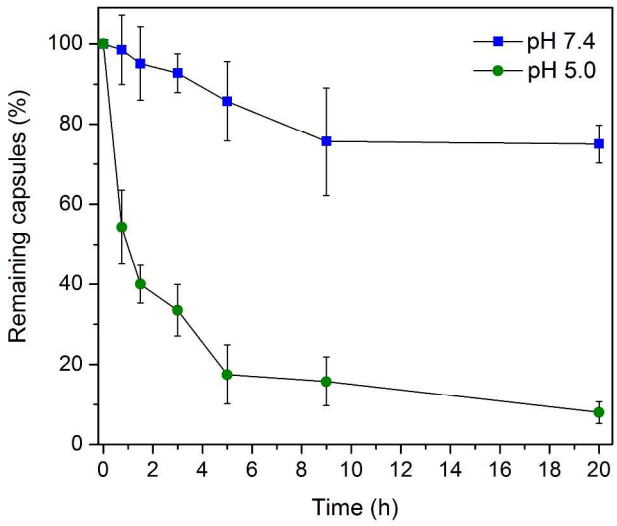

Figure 2. Flow cytometry analysis of the pH-responsive disassembly of PEG-MPN capsules. Error bars represent the standard deviation of three independent experiments.

pH-Dependent Disassembly of PEG-MPN Capsules. Intracellular drug delivery favors carriers that are stable at physiological pH and readily disassemble in the intracellular compartments with acidic pH, *e.g.*, lysosomes.[29] As the PEG-MPN capsules were cross-linked by coordination complexes between catechol groups of PEG-polyphenol and Fe^{III}, the stability of the capsules was expected to be pH-dependent due to the stoichiometric transitions of the PEG-polyphenol−Fe^{III} complexes. To examine the disassembly of PEG-MPN capsules, the capsules were incubated at pH 7.4 or 5.0 at 37 °C to mimic physiological and intracellular lysosomal environments, respectively. The number of remaining capsules was investigated *via* gating the population of the intact capsules using flow cytometry. At pH 7.4, more than 75% of the capsules were intact after 20 h (Figure 2), indicating slow disassembly of the capsules at physiological pH. In contrast, the number of remaining PEG-MPN capsules rapidly decreased at pH 5, with less than 20% intact capsules after 5 h of incubation. These data demonstrate the pH-dependent disassembly of PEG-MPN capsules due to the dissociation of the metal-catechol

coordination complexes. Utilization of catechol groups allows adjustment of the pH-disassembly profile of the MPN capsules to physiologically relevant acidic pH due to the pH-dependent stoichiometry of the PEG-polyphenol−Fe^{III} coordination complex (Figure S2). This rapid disassembly of PEG-MPN capsules is in stark contrast to MPN capsules with TA as a building block: TA-MPN capsules exhibit much slower disassembly at pH 5 (70% of capsules remain after 10 days) due to the high stability of TA−Fe^{III} coordination complexes.[6]

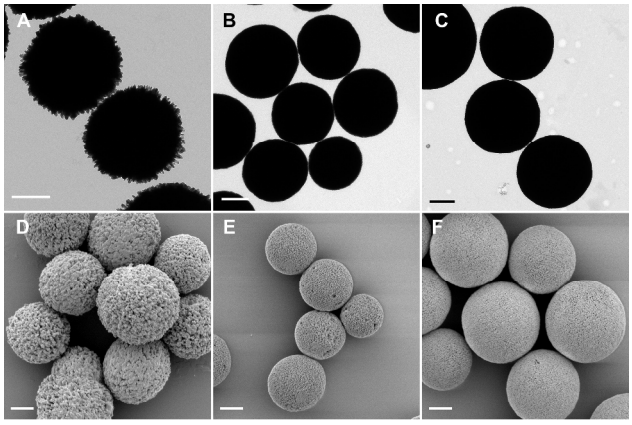

Figure 3. TEM images of (A) $CaCO_3$ templates, (B) BSA_{AF488}-loaded $CaCO_3$ templates, and (C) $dextran_{FITC}$-loaded $CaCO_3$ templates. SEM images of (D) $CaCO_3$ templates, (E) BSA_{AF488}-loaded $CaCO_3$ templates, and (F) $dextran_{FITC}$-loaded $CaCO_3$ templates. Scale bars are 1 μm.

Cargo Encapsulation of PEG-MPN Capsules. Encapsulation of biomacromolecules (*e.g.*, proteins) into capsules is of interest for drug delivery. Bovine serum albumin (BSA) and dextran were employed as models to assess the ability of PEG-MPN capsules to encapsulate cargo. Initially, AF488-labeled BSA (BSA_{AF488}) or FITC-labeled dextran ($dextran_{FITC}$, 2000 kDa) were preloaded in $CaCO_3$ templates *via* a co-precipitation method.[21] The successful preparation of $CaCO_3$ templates was confirmed by SEM and TEM (Figure 3). Notably, the $CaCO_3$ particles coprecipitated with BSA or dextran displayed smoother surfaces compared with the $CaCO_3$ particles prepared without additives, which suggests the loading of BSA or dextran. This is

consistent with a previous report showing the presence of BSA resulted in $CaCO_3$ particles composed of smaller nanoprecipitates.[21] PEG-MPN films then were deposited onto the cargo-loaded $CaCO_3$ templates by the subsequent addition of PEG-polyphenol and $FeCl_3$ solution. Monodisperse, spherical capsules were obtained after template removal, as observed by DIC microscopy (Figure 4A,F). After template removal, PEG-MPN capsules loaded with BSA_{AF488} and $dextran_{FITC}$ swelled slightly from 2.4 ± 0.2 µm to 2.9 ± 0.2 µm and from 3.5 ± 0.3 µm to 3.9 ± 0.3 µm, respectively. Successful encapsulation of the cargo (BSA_{AF488} or $dextran_{FITC}$) was demonstrated by fluorescence microscopy, which showed homogeneously distributed fluorescence within the capsules (Figure 4B,G). From TEM, SEM, and AFM images (Figure 4C-E,H-J), smoother surfaces of the capsules are visible and the contrast of these capsules is higher than that of non-cargo-loaded capsules. Furthermore, the single-layer thickness of cargo-loaded capsules is 27 ± 2 nm for BSA and 28 ± 2 nm for dextran (Figure S3), which are higher than the value determined for non-cargo-loaded capsules (20 ± 2 nm). This apparent increase in thickness can be attributed to cargo trapped inside the capsules.

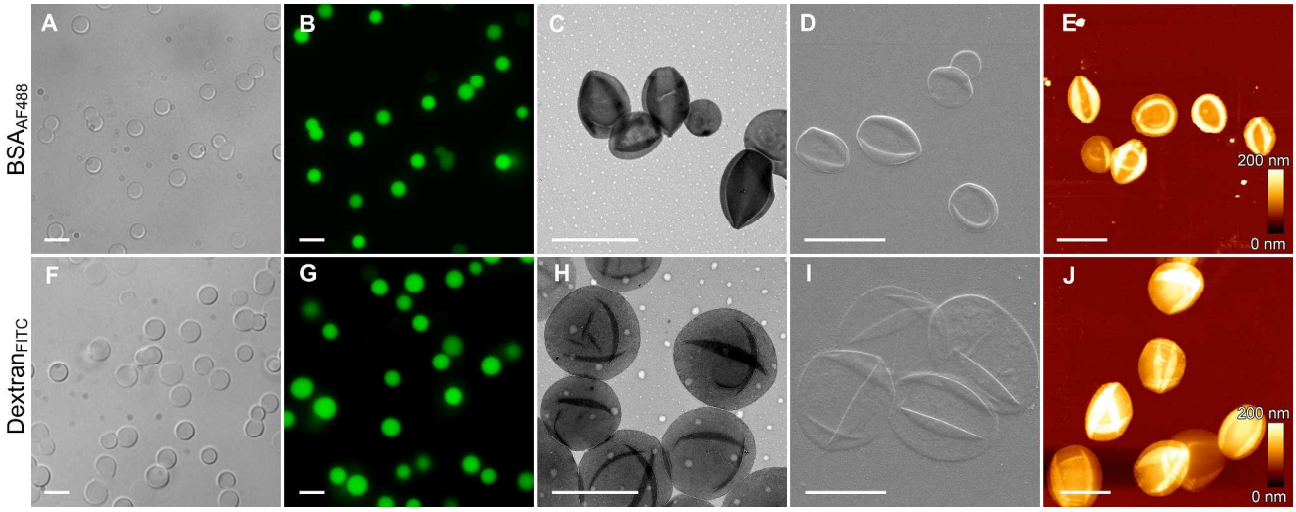

Figure 4. (A,F) DIC microscopy, (B,G) fluorescence microscopy, (C,H) TEM, (D,I) SEM, and (E,J) AFM images of PEG-MPN capsules loaded with BSA_{AF488} (top row) and $dextran_{FITC}$ (bottom row). Scale bars are 5 μm.

Cargo Release from PEG-MPN Capsules. As PEG-MPN capsules can encapsulate biomacromolecules and disassemble upon exposure to acidic pH, we investigated their pH-dependent cargo release. Unlabeled capsules were loaded with $dextran_{FITC}$ with a molecular weight of 2000 kDa. Prior to the experiment, we determined the $dextran_{FITC}$ loading based on the number of loaded PEG-MPN capsules and the concentration of $dextran_{FITC}$ by flow cytometry and fluorescence spectrophotometry, respectively. The amount of $dextran_{FITC}$ was 0.59 ± 0.03 pg per PEG-MPN capsule. To examine the pH-dependent release, $dextran_{FITC}$-loaded capsules were incubated at pH 7.4 or 5.0 at 37 °C with mild shaking. The fluorescence intensity of $dextran_{FITC}$-loaded capsules was monitored by flow cytometry. About 80% of $dextran_{FITC}$ remained encapsulated in the PEG-MPN capsules after 16 h of incubation (Figure 5). In contrast, at pH 5.0, around 90% of $dextran_{FITC}$ was released after 9 h of incubation, demonstrating the acid–pH-triggered release of cargo due to disassembly of the capsules. This encapsulation and triggered release of cargo suggests the potential use of PEG-MPN capsules as drug delivery carriers. We also performed release studies with BSA (Figure S6), where we found that release was faster at pH 7.4 compared with 5.0. This is partly attributed to the lower charge of BSA at pH 5 (isoelectric point of BSA=4.7), possibly because of the interaction between BSA and the phenolic networks.

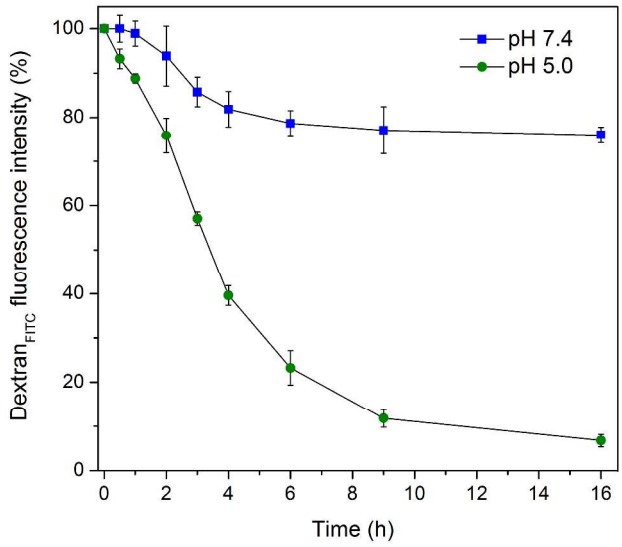

Figure 5. Release of encapsulated dextran$_{FITC}$ from PEG-MPN capsules at pH 7.4 and 5.0, respectively. The (normalized) fluorescence intensity from dextran$_{FITC}$ in PEG-MPN capsules was monitored by flow cytometry over 16 h. Error bars represent the standard deviation of three independent experiments.

Resistance to Nonspecific Protein Adsorption. Low fouling is a key requirement for drug delivery applications where a low level of nonspecific interactions with blood components is needed to allow carriers to have extended blood circulation.[30,31] PEG-MPNs are mainly comprised of PEG, which has well-demonstrated low-fouling properties, and is commonly applied as a stealth coating to biomedical implants and drug delivery carriers.[32-34] To assess the low-fouling properties of PEG-MPNs, protein adsorption of PEG-MPN thin films was first determined on planar substrates by quartz crystal microgravimetry (QCM). The coating of PEG-MPNs on gold chips resulted in a film coverage of 3.2 ± 0.4 ng mm^{-2}. PEG-MPN-coated gold chips were subsequently incubated with 100% human blood serum (HBS) for 1 h at 37 °C, followed by washing with PBS and Milli-Q water to remove the non-adsorbed protein. For comparison, TA-MPN, PEI, and PMA films were examined under the same conditions. After

incubation, the amount of adsorbed protein was calculated using the Sauerbrey equation,[23] which relates the resonant frequency decrease (measured by QCM) to the increase in protein adsorption. TA-MPN-coated gold chips exhibited a 158 ± 10 Hz reduction in resonant frequency (Figure S7), corresponding to a protein adsorption of 8.6 ± 0.5 ng mm^{-2}. In contrast, the amount of proteins adsorbed on PEG-MPN films was about five-fold less (1.8 ± 0.2 ng mm^{-2}), showing that compared with the TA-MPN films, PEG-MPN films exhibited significantly improved resistance to nonspecific protein adsorption. Compared with PEG-MPN films, positively charged PEI films and negatively charged PMA films exhibited about seven-fold (11.8 ± 0.7 ng mm^{-2}) and three-fold (4.6 ± 0.5 ng mm^{-2}) more protein adsorption, respectively.

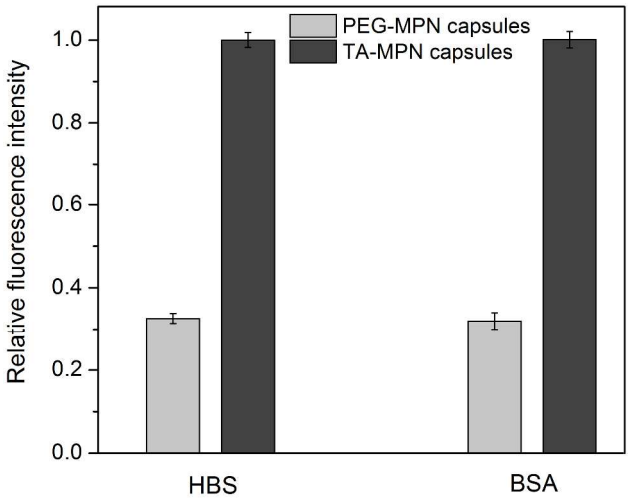

Figure 6. Protein adsorption study of PEG-MPN capsules and TA-MPN capsules, evaluated by flow cytometry. The unlabeled capsules were incubated with AF488-labeled human blood serum (HBS, 50% in PBS) or bovine serum albumin (BSA, 5 mg mL^{-1} in PBS) for 1 h, followed by washing with PBS three times. Error bars represent the standard deviation of three independent experiments.

To examine whether the low-fouling properties of planar PEG-MPN films would also apply to PEG-MPNs of spherical geometry, we further investigated the protein adsorption of PEG-MPN

capsules. Similar to the experiments performed on planar surfaces, PEG-MPN and TA-MPN capsules were incubated with AF488-labeled HBS (50% in PBS) or AF488-labeled BSA (5 mg mL-1 in PBS) for 1 h at 37 °C. The fluorescence intensity of capsules, corresponding to the relative amount of protein adsorbed on the capsules, was measured by flow cytometry. It was found that PEG-MPN capsules had three times less HBS or BSA adsorbed than TA-MPN capsules (Figure 6). The results were consistent with the findings on planar films, highlighting the lower fouling property of the PEG-MPN system.

Resistance to Nonspecific Cellular Association. To further examine the low-fouling properties of PEG-MPNs in a biological environment, PEG-MPN capsules were incubated with HeLa cells at a capsule-to-cell ratio of 50:1 and the cell association of the capsules was evaluated using flow cytometry and deconvolution microscopy. HeLa cells were chosen to investigate the cell association, as they are one of the most commonly used cell lines for *in vitro* studies.[35] For comparison, TA-MPN capsules were also investigated under the same conditions. PEG-MPN and TA-MPN capsules were fluorescently labeled by loading BSA_{AF488}. After 4 h of incubation, cell association of TA-MPN capsules was about 41% and increased with longer incubation times (Figure 7A). In contrast to TA-MPN capsules, the cell association of PEG-MPN capsules was very low (below 2%), even after 24 h incubation; this indicates PEG-MPN capsules are resistant to nonspecific cell interaction. To confirm these results, deconvolution microscopy analysis was performed after 24 h incubation. As expected, there was a significant number of TA-MPN capsules associated with or internalized by HeLa cells (Figure 7C), while no PEG-MPN capsules were associated with cells (Figure 7B). Such significant resistance to nonspecific cellular interactions may render PEG-MPN capsules promising candidates for drug delivery applications.

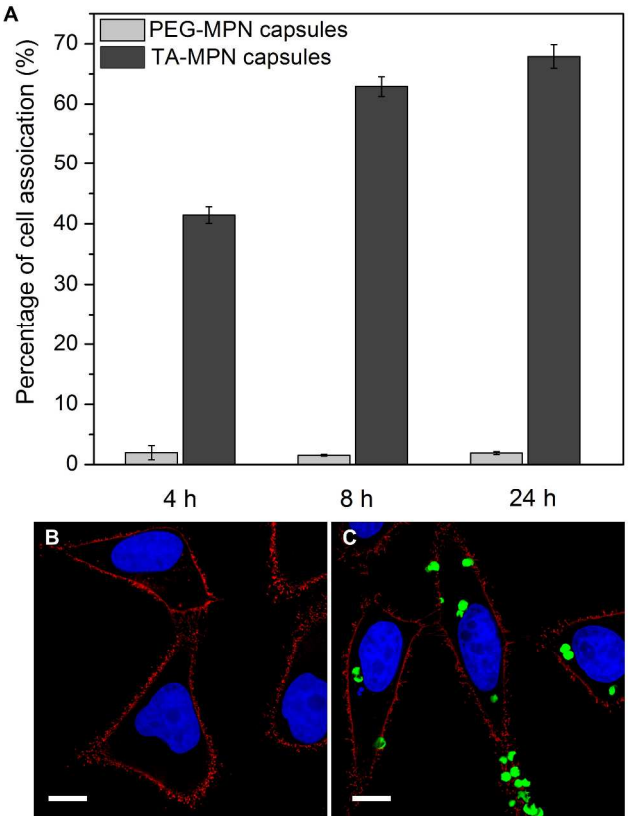

Figure 7. (A) Flow cytometry analysis of HeLa cells associated with BSA_{AF488}-loaded PEG-MPN capsules or BSA_{AF488}-loaded TA-MPN capsules, after 4 h, 8 h, and 24 h incubation at 37 °C. Error bars represent the standard deviation of three independent experiments. Representative deconvolution microscopy images of HeLa cells incubated with (B) BSA_{AF488}-loaded PEG-MPN capsules or (C) BSA_{AF488}-loaded TA-MPN capsules, after 24 h incubation at 37 °C. Cell membranes and nuclei were stained with WGA594 (red) and Hoechst 33342 (blue), respectively. Green fluorescence represents TA-MPN capsules loaded with BSA_{AF488}. Scale bars are 10 μm. The capsule-to-cell ratio was adjusted to 50:1 for all cell experiments.

CONCLUSIONS

We have demonstrated a facile strategy to assemble low-fouling PEG capsules by combining the properties of a synthetic polymer (PEG) with the advantages of metal-phenolic coordination chemistry. Using a synthetic PEG-polyphenol, the PEG-MPN capsules can be rapidly assembled

at alkaline pH due to the high surface binding and metal chelating ability of phenolic groups. The PEG-MPN capsules disassemble and release encapsulated cargo at a physiologically relevant acidic pH (5). In addition, the low-fouling PEG backbones endowed the capsules with low nonspecific protein adsorption and cell association properties. The reported PEG-MPN capsules provide a platform for future drug delivery and related bio-applications.

ASSOCIATED CONTENT

Supporting Information

^{1}H-NMR spectrum, UV-Vis absorption spectra, AFM height profiles, EDX spectrum, and QCM measurement. This material is available free of charge *via* the Internet at http://pubs.acs.org.

AUTHOR INFORMATION

Corresponding Author

* Email: fcaruso@unimelb.edu.au

Notes

The authors declare no competing financial interest.

ACKNOWLEDGMENT

This work was conducted and funded by the Australian Research Council Centre of Excellence in Convergent Bio-Nano Science and Technology (project number CE140100036). This work was also supported by Australian Research Council under the Australian Laureate Fellowship (F.C., FL120100030) and Super Science Fellowship (F.C., FS110200025) schemes. M.M. acknowledges The University of Melbourne for a McKenzie Fellowship. Deconvolution imaging

was performed by Benjamin Hibbs at the Materials Characterisation and Fabrication Platform (MCFP). We thank Dr. Kristian Kempe, Dr. Huanli Sun, Dr. Julia Braunger and Junling Guo for helpful discussions.

REFERENCES

(1) Tanner, P.; Baumann, P.; Enea, R.; Onaca, O.; Palivan, C.; Meier, W. *Acc. Chem. Res.* **2011**, *44*, 1039−1049.

(2) Lensen, D.; Vriezema, D. M.; van Hest, J. *Macromol. Biosci.* **2008**, *8*, 991−1005.

(3) van Dongen, S. F.; de Hoog, H.-P. M.; Peters, R. J.; Nallani, M.; Nolte, R. J.; van Hest, J. C. *Chem. Rev.* **2009**, *109*, 6212−6274.

(4) De Cock, L. J.; De Koker, S.; De Geest, B. G.; Grooten, J.; Vervaet, C.; Remon, J. P.; Sukhorukov, G. B.; Antipina, M. N. *Angew. Chem. Int. Ed.* **2010**, *49*, 6954−6973.

(5) Yan, Y.; Björnmalm, M.; Caruso, F. *ACS Nano* **2013**, *7*, 9512−9517.

(6) Ejima, H.; Richardson, J. J.; Liang, K.; Best, J. P.; van Koeverden, M. P.; Such, G. K.; Cui, J.; Caruso, F. *Science* **2013**, *341*, 154−157.

(7) Lomova, M. V.; Sukhorukov, G. B.; Antipina, M. N. *ACS Appl. Mater. Interfaces* **2010**, *2*, 3669-3676.

(8) Kozlovskaya, V.; Kharlampieva, E.; Drachuk, I.; Cheng, D.; Tsukruk, V. V. *Soft Matter* **2010**, *6*, 3596-3608.

(9) Guo, J.; Ping, Y.; Ejima, H.; Alt, K.; Meissner, M.; Richardson, J. J.; Yan, Y.; Peter, K.; von Elverfeldt, D.; Hagemeyer, C. E.; Caruso, F. *Angew. Chem. Int. Ed.* **2014**, *53*, 5546−5551.

(10) Sileika, T. S.; Barrett, D. G.; Zhang, R.; Lau, K. H. A.; Messersmith, P. B. *Angew. Chem. Int. Ed.* **2013**, *52*, 10766−10770.

(11) Spencer, C. M.; Cai, Y.; Martin, R.; Gaffney, S. H.; Goulding, P. N.; Magnolato, D.; Lilley, T. H.; Haslam, E. *Phytochemistry* **1988**, *27*, 2397−2409.

(12) Siebert, K. J.; Troukhanova, N. V.; Lynn, P. Y. *J. Agric. Food Chem.* **1996**, *44*, 80−85.

(13) Williamson, M. P.; McCormick, T. G.; Nance, C. L.; Shearer, W. T. *J. Allergy Clin. Immunol.* **2006**, *118*, 1369−1374.

(14) Shutava, T. G.; Balkundi, S. S.; Lvov, Y. M. *J. Colloid Interface Sci.* **2009**, *330*, 276-283.

(15) Hong, S.; Yang, K.; Kang, B.; Lee, C.; Song, I. T.; Byun, E.; Park, K. I.; Cho, S. W.; Lee, H. *Adv. Funct. Mater.* **2013**, *23*, 1774−1780.

(16) Wei, Q.; Achazi, K.; Liebe, H.; Schulz, A.; Noeske, P.-L. M.; Grunwald, I.; Haag, R. *Angew. Chem. Int. Ed.* **2014**, *53*, 11650−11655.

(17) Holten-Andersen, N.; Harrington, M. J.; Birkedal, H.; Lee, B. P.; Messersmith, P. B.; Lee, K. Y. C.; Waite, J. H. *Proc. Natl. Acad. Sci. U.S.A.* **2011**, *108*, 2651−2655.

(18) Vllasaliu, D.; Fowler, R.; Stolnik, S. *Expert Opin. Drug Deliv.* **2014**, *11*, 139−154.

(19) Otsuka, H.; Nagasaki, Y.; Kataoka, K. *Adv. Drug Delivery Rev.* **2003**, *55*, 403−419.

(20) Volodkin, D. V.; Larionova, N. I.; Sukhorukov, G. B. *Biomacromolecules* **2004**, *5*, 1962−1972.

(21) Petrov, A. I.; Volodkin, D. V.; Sukhorukov, G. B. *Biotechnol. Prog.* **2005**, *21*, 918−925.

(22) Tjipto, E.; Quinn, J. F.; Caruso, F. *Langmuir* **2005**, *21*, 8785−8792.

(23) Sauerbrey, G. *Z. Phys.* **1959**, *155*, 206−222.

(24) Mizrahi, B.; Khoo, X.; Chiang, H. H.; Sher, K. J.; Feldman, R. G.; Lee, J.-J.; Irusta, S.; Kohane, D. S. *Langmuir* **2013**, *29*, 10087−10094.

(25) Lee, B. P.; Dalsin, J. L.; Messersmith, P. *Polym. Prepr. (Am. Chem. Soc., Div. Polym. Chem.)* **2001**, *42*, 151−152.

(26) Huang, K.; Lee, B. P.; Ingram, D. R.; Messersmith, P. B. *Biomacromolecules* **2002**, *3*, 397−406.

(27) Sever, M. J.; Wilker, J. J. *Dalton Trans.* **2004**, 1061−1072.

(28) Lee, H.; Dellatore, S. M.; Miller, W. M.; Messersmith, P. B. *Science* **2007**, *318*, 426−430.

(29) Delcea, M.; Möhwald, H.; Skirtach, A. G. *Adv. Drug Delivery Rev.* **2011**, *63*, 730−747.

(30) Amoozgar, Z.; Yeo, Y. *Wiley Interdiscip. Rev. Nanomed. Nanobiotechnol.* **2012**, *4*, 219−233.

(31) Chen, S.; Li, L.; Zhao, C.; Zheng, J. *Polymer* **2010**, *51*, 5283−5293.

(32) Veronese, F. M.; Pasut, G. *Drug Discovery Today* **2005**, *10*, 1451−1458.

(33) Müllner, M.; Cui, J.; Noi, K. F.; Gunawan, S. T.; Caruso, F. *Langmuir* **2014**, *30*, 6286−6293.

(34) Kim, H. S.; Ham, H. O.; Son, Y. J.; Messersmith, P. B.; Yoo, H. S. *J. Mater. Chem. B* **2013**, *1*, 3940−3949.

(35) Yan, Y.; Such, G. K.; Johnston, A. P.; Best, J. P.; Caruso, F. *ACS Nano* **2012**, *6*, 3663−3669.

Table of Contents entry